

# Synthesis and Characterisation of ZnO–Ag Thin Films and Their use as Ammonia Sensors

Mohammed Bandr Abdullwahed<sup>1</sup>, Ahmed Mishaal Mohammed<sup>2\*</sup>, Firas Fadhel Ali<sup>3</sup>

<sup>1,2</sup> Department of Chemistry, College of Science, University Of Anbar, Ramadi, Iraq.

<sup>3</sup> Department of Chemistry, College of Education for women, University Of Anbar, Ramadi, Iraq.

Corresponding author:

**Ahmed Mishaal Mohammed**

sc.dr.ahmedm.mohammed@uoanbar.edu.iq

## Abstract

This study involves the preparation of colloidal silver (Ag) nanoparticle solution using Turkevich method. Specifically, the solution is mixed with the zinc nitrate hexahydrate and hexamethylenetetramine solution with various volume ratios (e.g. 50, 70 and 90 AgNPs %V) to deposit zinc oxide (ZnO)–Ag thin films on glass substrates at 350 °C using chemical spray pyrolysis technique. Then, these thin films are used to measure the sensitivity of ammonia (NH<sub>3</sub>) at room temperature (30 °C–32 °C). The thin films formed by this technique have been characterised by the following measurements: FE-SEM, XDR, AFM and EDXA; whereas, AFM, UV-Visible spectrophotometer and FT-IR spectrophotometer have been used to characterise the prepared Ag nanoparticles. The average size of ZnO–Ag nanoparticles formed on glass substrates is within the range of 68.93–86.64 nm, whereas the average size of Ag nanoparticles formed through Turkevich method is 48.9 nm. The XRD measurements show the wurtzite hexagonal and face centred cubic crystal structure of ZnO and Ag, respectively. The thin film that contains 50 %V of Ag has the highest gas sensitivity (69%). The high sensitivity of the ZnO–Ag sensor at room temperature is an indicator of the high efficiency of NH<sub>3</sub> gas sensing.

**Keywords:** Gas sensor, NH<sub>3</sub>, AgNPs, Turkevich, ZnO

## 1. Introduction

Numerous gases, such as ammonia (NH<sub>3</sub>), carbon monoxide (CO), sulphur dioxide (SO<sub>2</sub>), nitrogen oxide (NO<sub>x</sub>) and hydrogen sulphide (H<sub>2</sub>S), are considered toxic and polluting to the environment. These gases are a major concern for researchers [1-3]. NH<sub>3</sub> is a colourless, explosive, hazardous and flammable gas accompanied by pungent odour. NH<sub>3</sub> gas has a harmful effect on the throat, eyes and respiratory and pulse rates. It can also cause oedema of the lungs, permanent blindness and death upon prolonged exposure. This gas is produced in our environment from countless industrial sources, such as fertilizers, textiles, refrigeration, different chemicals, food processing industries, fire power plants and pesticides [4-8]. Therefore, NH<sub>3</sub> production has become important in the development of sensors for explosive and toxic gases that are considered sources of leaks and spills; it is also well-known for its use

in environmental monitoring and food quality control [9,10], industries, medical diagnosis, and agriculture [11].

Zinc oxide (ZnO) nanoparticles are used in different applications, such as UV sensors [12], transparent electrodes [13], optoelectronic devices [14], gas sensors [15,16], transducers [17] and solar cells [18]. In terms of gas sensing application, ZnO nanomaterials have been used for detecting and reducing oxidative gases with good performance, such as NH<sub>3</sub> [19], NO<sub>2</sub> [20], LPG [21], H<sub>2</sub> [22] and acetylene [23]. ZnO-based sensors are more preferred than other metal oxide-based conductive sensors to gas species because of their low cost, high sensitivity, ease of fabrication [24], long-term stability, short response–recovery time, fast response and excellent electrical performance [25-27].

Doping with noble metals, such as Ag [28–30], Ni, Pd, Pt [31–33] and Au [29], improves the electronic properties and increases the surface area of the ZnO nanoparticles, which are considered extremely important for enhanced gas sensor applications [34]. Ag nanoparticles can improve their gas-sensing performance greatly because it can accelerate the chemisorption process of metal oxides [35].

Various methods, such as spray pyrolysis [36,37], pulsed laser deposition [38] and sol–gel [39], can be used to synthesise ZnO films. Spray pyrolysis is a simple method that can be used to prepare thin films by spraying a solution on a preheated surface, wherein a chemical compound is formed through the reaction of the constituents. Spray pyrolysis is firstly used in 1966 to prepare a CdS-made thin film [40-42]. This method has many advantages [36], including its simplicity in doping the prepared films by adding any element in any proportion to the spray solution [43], does not require vacuum (evacuation) at any stage (vacuum conditions are not required) [44], does not require high-quality chemicals or substrates [45] and the thickness of the prepared films can be easily controlled by changing the parameters of spray process [46]. Accordingly, this research aims to prepare ZnO–Ag thin films using NH<sub>3</sub> gas sensors.

## **2. Materials and Methods**

### **2.1 Chemicals**

Zinc nitrate hexahydrate Zn(NO<sub>3</sub>)<sub>2</sub>·6H<sub>2</sub>O, Ethanol C<sub>2</sub>H<sub>5</sub>OH, hexamethylenetetramine C<sub>6</sub>H<sub>12</sub>N<sub>4</sub> and silver (Ag) nitrate AgNO<sub>3</sub> were commercially purchased from Sigma–Aldrich. Trisodium citrate Na<sub>3</sub>C<sub>6</sub>H<sub>5</sub>O<sub>7</sub> was purchased commercially from AppliChem GmbH in Germany. All these chemicals were used as received from the abovementioned manufacturers without using any additional purification.

### **2.2 Preparation of spray solutions**

**1.** Solution A: AgNO<sub>3</sub> (0.1275 g) was dissolved in 250 ml of deionised water under continuous stirring and heated at 85 °C (±3) using a hotplate stirrer. Then, 25 ml of trisodium citrate (2%) was added slowly (Fig. 1).

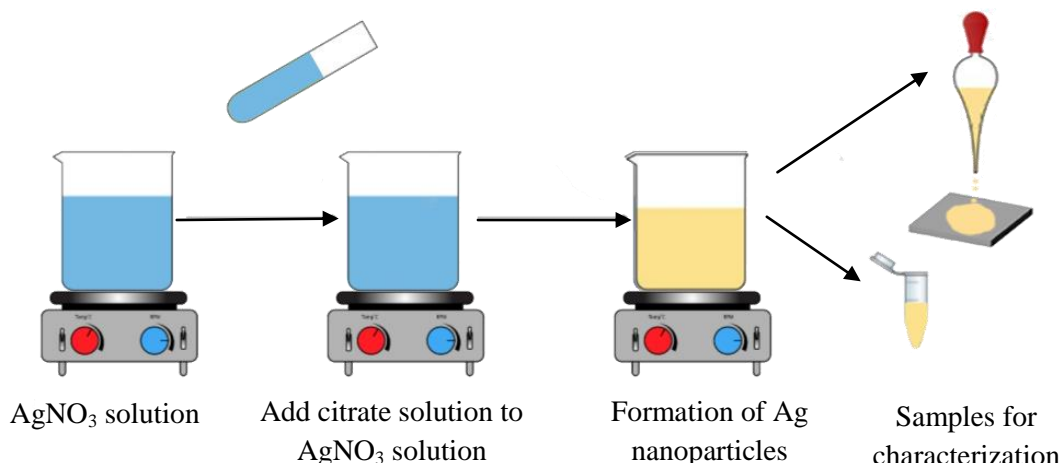
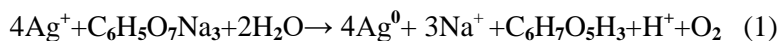


Fig. 1: Scheme of silver nanoparticles preparation

The golden-yellow colour was observed (i.e. an indication of Ag nanoparticles) after the addition of trisodium citrate solution (typically 6–7 min after addition). The hot plate stirrer was turned off, and the coloured solution was removed to cool it at room temperature for later use. Several drops of this solution were dispersed on clean glass substrate and dried in oven at 60 °C to gain the AFM and XRD data of the prepared Ag nanoparticles. Ag nanoparticles were formed according to Eq. 1 [47,48].



2. Solution B: 1 g of Zn(NO<sub>3</sub>)<sub>2</sub>·6H<sub>2</sub>O and 10 g of C<sub>6</sub>H<sub>12</sub>N<sub>4</sub> were dissolved in 200 ml of deionised water and heated under continuous stirring using a hotplate stirrer to 50 °C for 1 hour to be more homogenous and ready for the spraying process. This solution formed the ZnO nanoparticles during spraying process (Eqs. 2–5) [49].



### 2.3 Synthesis of thin films

Firstly, the glass substrates are cleaned successively using detergent to remove grease and oils over the surface. Secondly, they are ultrasonically cleaned by ethanol for 20 min, followed by washing with deionised water. The glass substrates are then dried using a hot oven to prepare it for use. The homemade spray pyrolysis system was used to deposit ZnO–Ag thin films on the preheated glass substrates by using an aqueous solution as a precursor. This aqueous solution is composed of (A) and (B) solutions with various solution volume ratios listed in Table 1. The scheme diagram of the homemade spray pyrolysis unit in our study is shown in Fig. 2. Compressed air is used as a carrier gas to carry the precursor to the spray nozzle to spray it into the preheated substrate. Crystalline growth was observed on ZnO–Ag thin films because of nucleation, and thermal decomposition

reaction occurred when the spray solution dropped and reached the hot substrates. After depositing the thin films successfully, the prepared thin films are annealed inside the furnace in air atmosphere for 3 hours at 500 °C. Various parameters associated with the thin-film deposition process are listed in Table 2.

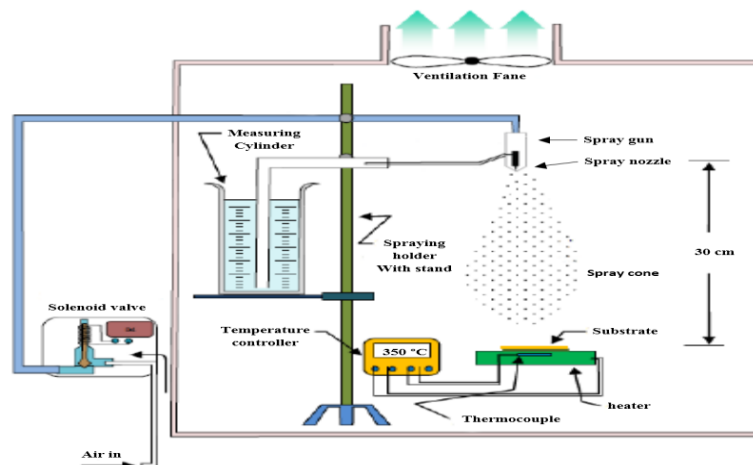


Fig.2: The scheme of the homemade spray pyrolysis system experimental setup used in our study

Table. 1: Various solution volumes ratios used in our study

Thin film symbol	Volumes ratios		Volume of (B)solution	Volume of solution (A)	Total volume
	Solution ratio (B)	Solution ratio (A)			
C1	10%	90%	10 ml	90 ml	100 ml
C2	30%	70%	30 ml	70 ml	100 ml
C3	50%	50%	50 ml	50 ml	100 ml

Table 2: The parameters associated with the thin film deposition process

Spray parameters	Optimum item/value
Substrate temperature	350±15 °C
Carrier gas	Compressed air
Nozzle	Stainless steel
Solvent	Deionized water
Substrate - nozzle distance	30 cm
Solution spray rate	13 ml/min
substrate	Glass
Spray time	9 Sec.
Time interval between sequent sprays	9 Sec.

## 2.4 Sensor fabrication

To fabricate the sensor device, a metal mask was fixed on the surface of the thin films deposited on the glass substrates. Then, the substrates were placed in the high vacuum physical vapour deposition system to deposit two aluminium electrodes on the thin-film surface (Fig. 3). The homemade gas sensing system (Fig. 4) was used to determine the gas sensitivity measurements of the ZnO–Ag thin films. The fabricated sensors were tested at different concentrations of NH<sub>3</sub> gas (50, 100 and 150 ppm) at room temperature. The gas sensitivity (S%) of fabricated sensors was calculated through Eq. (6) [50].

$$S\% = (R_a - R_g / R_a) \times 100, \quad (6)$$

where  $R_a$  is the electrical resistance of thin film in fresh air, and  $R_g$  is the electrical resistance of thin films after test gas exposure.

The response and recovery times were calculated through sensitivity plot. These measurements were defined as the time required for the sensing element to achieve 90% and 10% of the change in resistance from its original resistance [51,52].

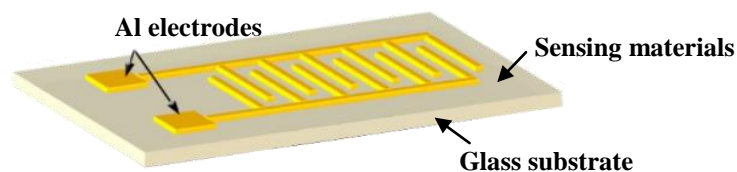


Fig. 3 A schematic of the patterned aluminum electrodes

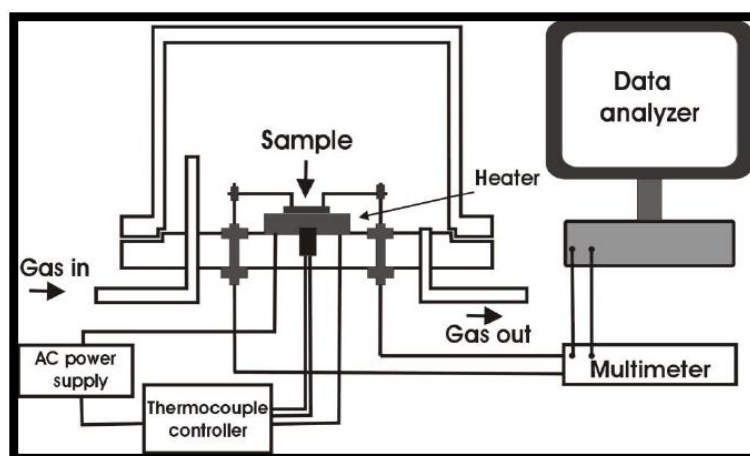


Fig. 4: A schematic of homemade gas sensing system

## 2.5 Characterisations and measurements

The existing elements, crystal planes and crystallinity of Ag and ZnO–Ag nanoparticles thin films were investigated by using X-ray diffractometer (XRD) (SHEMADZU-600-Japan) with Cu–K $\alpha$  radiation ( $\lambda = 1.5405 \text{ \AA}$ ) with a range of  $10^\circ$ – $80^\circ$ . The morphology and composition of ZnO–Ag thin films were investigated by using atomic force microscopy (AFM) (CSPM-USA) and field emission scanning electron microscopy (FE-SEM) (FEI NovaSEM 450-USA) coupled with EDS. The morphology of prepared Ag nanoparticles was examined by scanning electron microscopy (SEM) (Hitachi-S 4160-Japan) and atomic force microscopy (AFM) (CSPM-USA). The absorbance measurements of Ag nanoparticle solution and prepared thin films were obtained by using spectrophotometer (UV-Vis) (Jenway-USA) with a range of 300–600 nm and 300–700 nm,

respectively. The vibration modes of the functional group of Ag nanoparticles solution were recorded through Fourier transformation infrared (FT-IR) spectra (Bruker–Germany) using KBr pellets with a range of 400–4000  $\text{cm}^{-1}$ . The gas sensitivity of ZnO–Ag sensors was examined using a homemade test system.

### 3. Results and discussion

#### 3.1 XRD

The observed diffraction peaks at 002, 110, 102 and 100 planes in the XRD patterns (Figs. 5–7) belong to the wurtzite hexagonal phase of ZnO when compared with JCPDS data file no. 00-036-1451 [53,54]. The observed diffraction peaks in the obtained XRD patterns (Figs. 5–8) at 111, 220, 311 and 200 planes belong to face-centred cubic phase of Ag when compared with JCPDS data file no. 00-004-0783 [55].

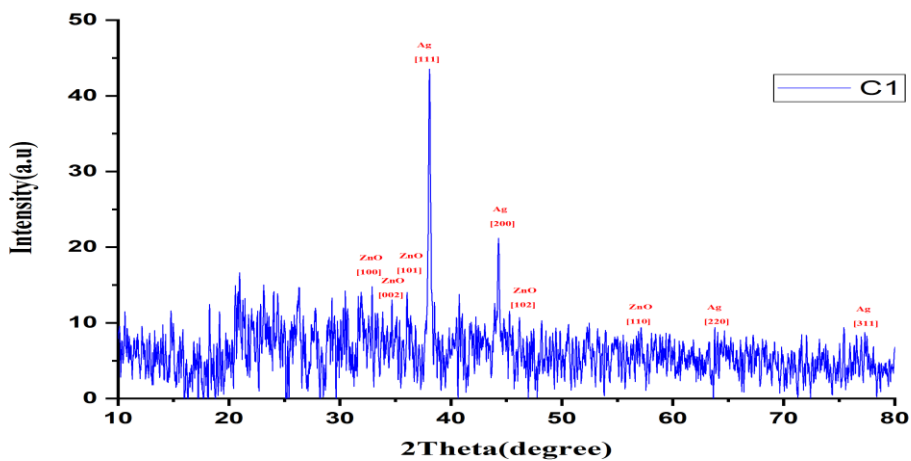


Fig. 5: XRD of (C1) thin film

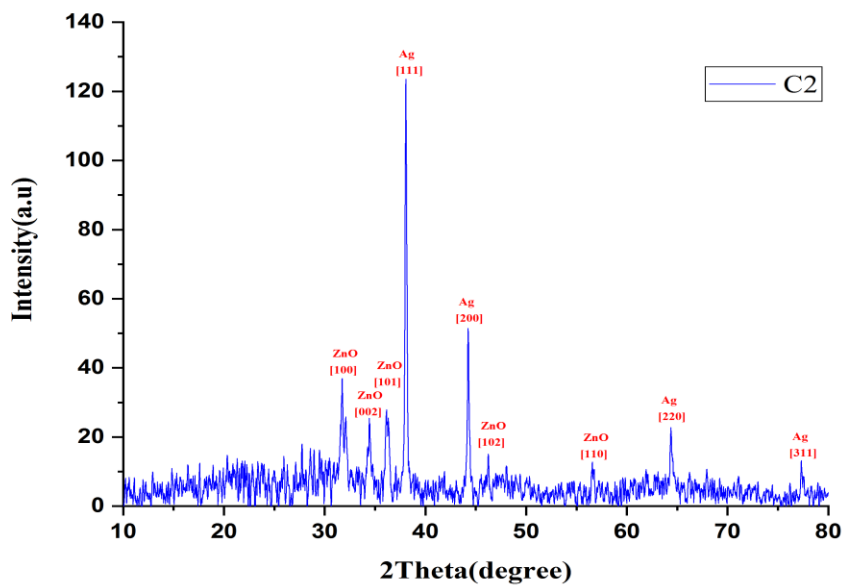


Fig. 6: XRD of (C2) thin film

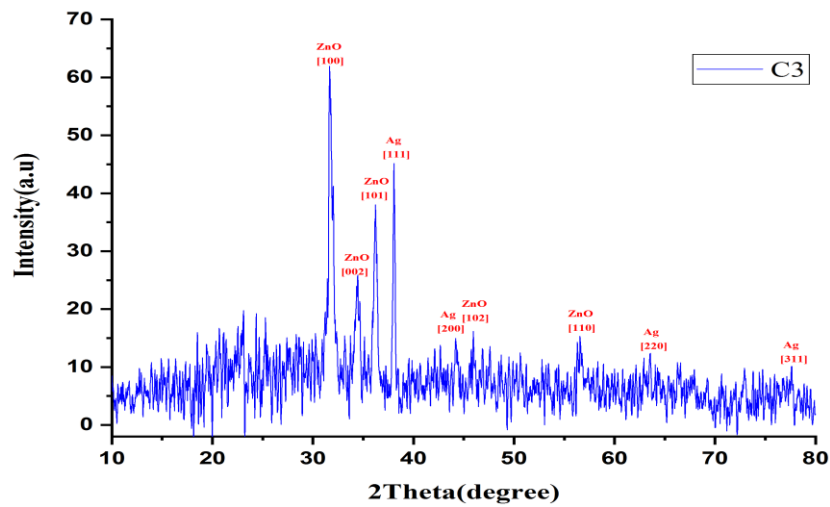


Fig. 7: XRD of (C3) thin film

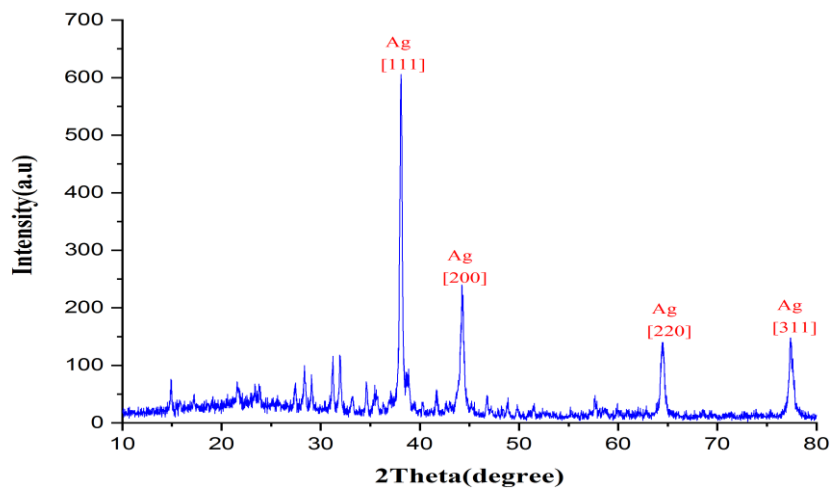


Fig. 8: XRD of AgNPs solution

### 3.2 FESEM and EDXA analysis

The surface morphology of the films is important given the key role it plays in gas sensing applications [56]. The high-resolution FESEM image of C2 thin film (Fig. 9) shows that ZnO has a nanoneedle structure, which agrees with Yas Al-Hadeethi et al.'s [28] research results. In addition to the sodium produced from the trisodium citrate (reducing agent) used to reduce Ag ions and the other impurities that appeared, Fig. 10 shows that the EDXA spectra of C2 thin film, which contains ZnO and Ag, may have come from materials that are used for manufacturing glass substrates.

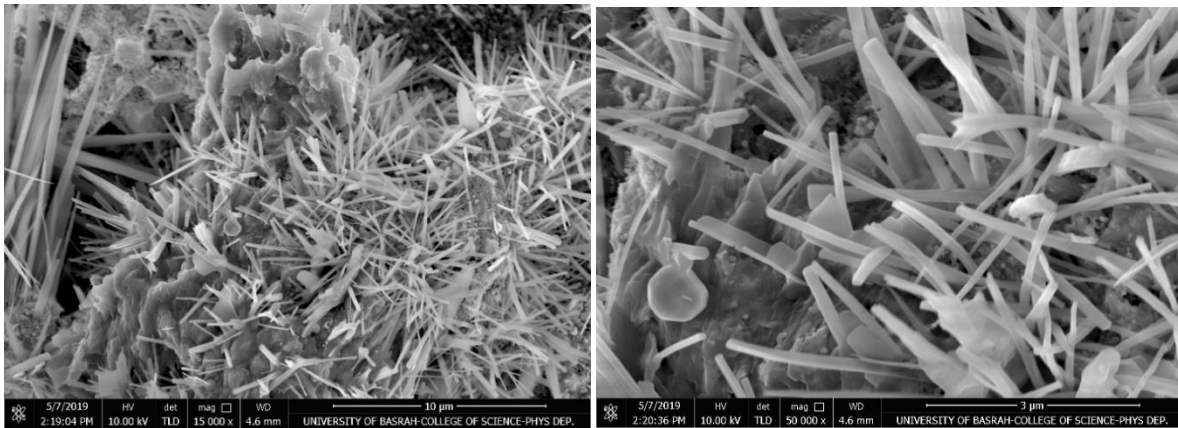


Fig. 9: FE-SEM (C2) thin film

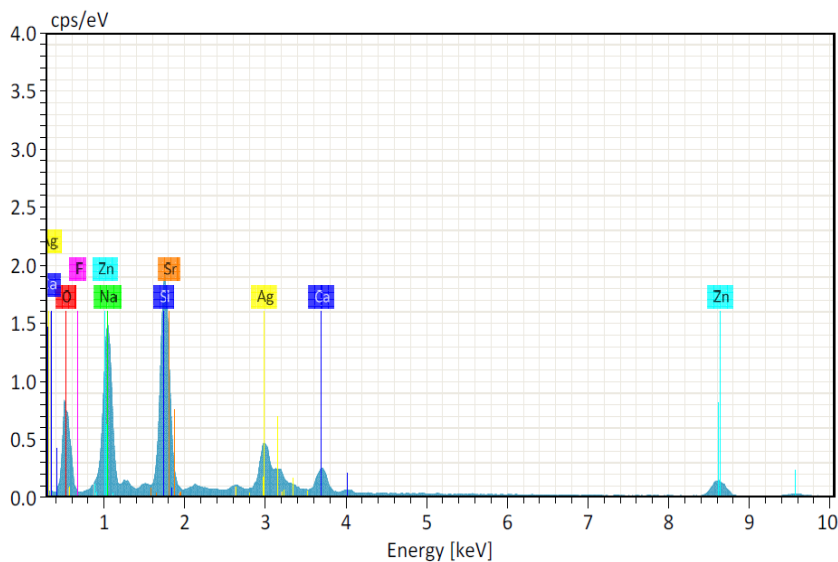


Fig. 10: EDXA spectra of (C2) thin film

### 3.3 AFM

The form of the prepared thin films was investigated using AFM. Surface roughness and particle size play important roles in the interaction of gases within the surface [57]. AFM images of C1, C2 and C3 thin films deposited on glass substrates are shown in Fig. 11. These images have a highly regular and homogeneous granular distribution. The C1, C2 and C3 films obtained the following results: root mean square (RMS) of 7.65, 5.22 and 8.88 nm, respectively; average grain size of 81.17, 68.93 and 86.64 nm, respectively; and average roughness of 6.68, 4.52 and 7.66 nm, respectively. The AFM image of dried AgNPs on the glass substrate has an average grain size of 48.9 nm (Fig. 12).



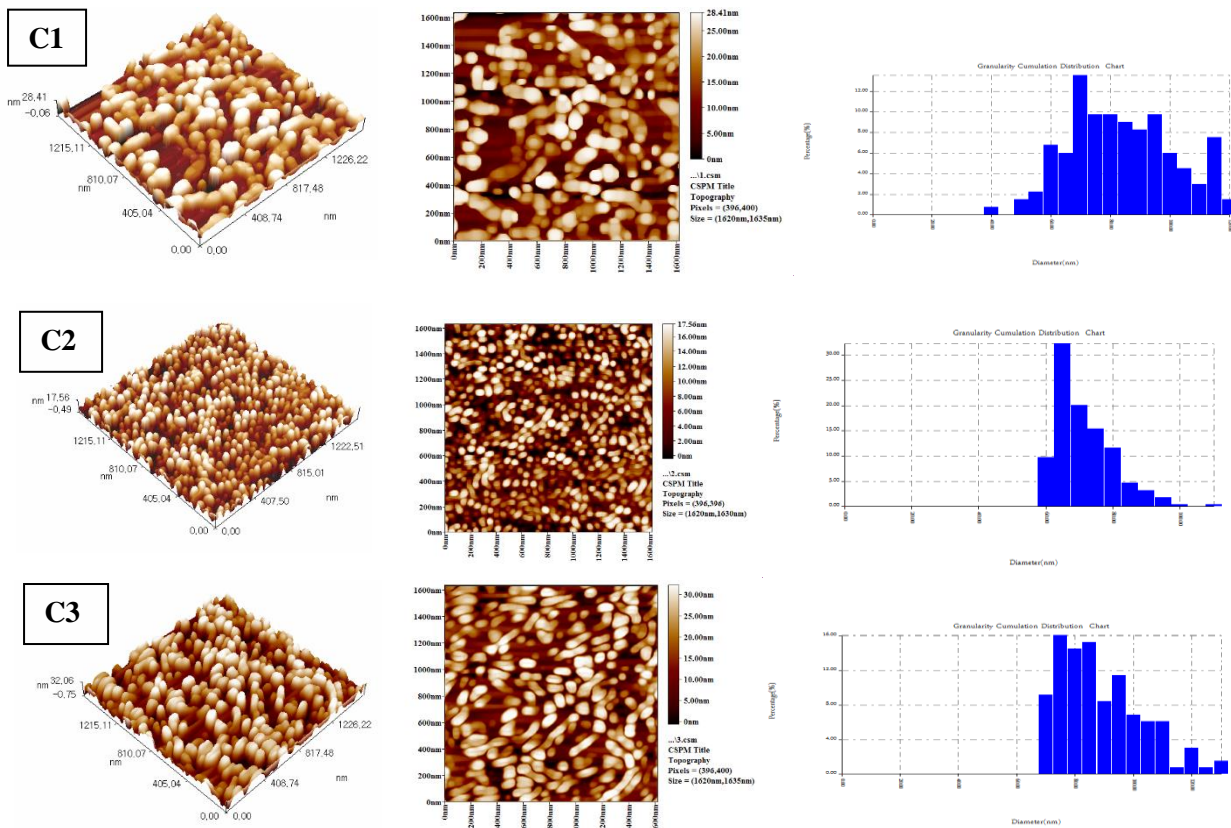


Fig. 11: AFM images of C1, C2 and C3 thin films

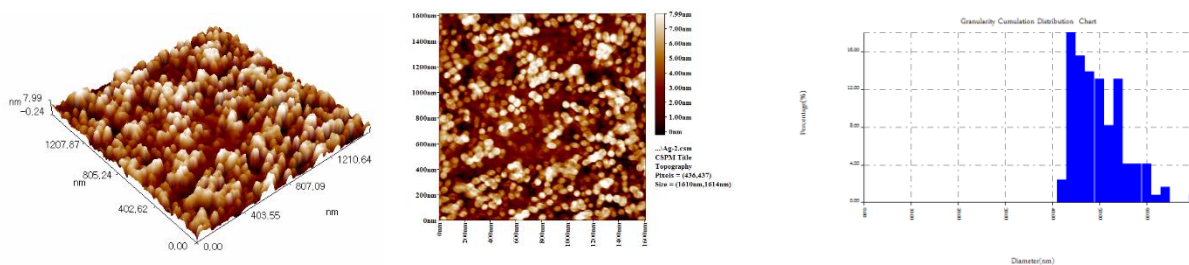


Fig. 12: AFM images of AgNPs

### 3.4 UV-Vis measurements

Figs. 13 and 14 show the recorded UV-Visible spectra of the deposited thin films and colloidal Ag nanoparticles, respectively. These recorded spectra have good agreement with Ismail and Shameli's research results [58, 59]. The decreasing intensity of the peaks in UV-Visible spectra (Fig. 13) from C1 to C3 thin films is due to the difference in the percentage of Ag nanoparticles in these films.

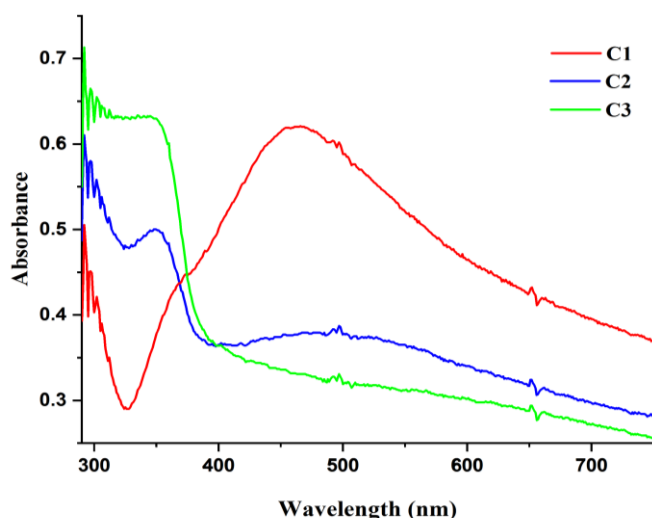


Fig. 13: UV-Vis spectra of C1, C2 and C3 thin films

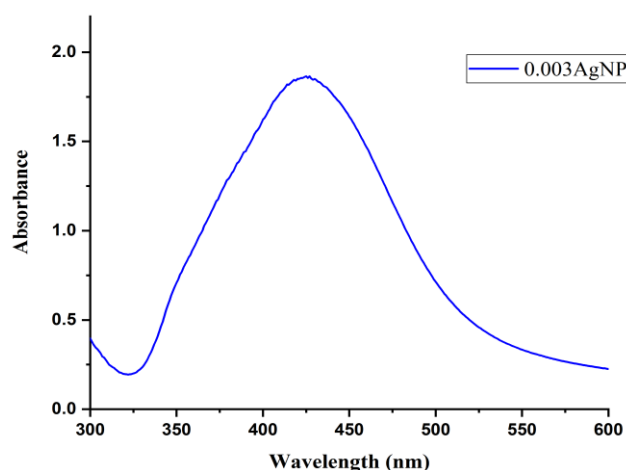


Fig. 14: UV-Vis spectra of AgNPs solution

### 3.5 FT-IR spectra of AgNPs solution

FT-IR spectroscopy can be applied to the gain information about functional groups of stabilisation and capping of the nanoparticles through peak positions in the spectrum. A drop of colloidal Ag nanoparticles was placed between two NaCl plates and in FT-IR spectrophotometer to scan within a range of  $4000\text{--}400\text{ cm}^{-1}$ . The FT-IR spectra of the prepared Ag nanoparticles are shown in Fig. 15. The peaks around  $1400\text{ cm}^{-1}$  and  $1600\text{ cm}^{-1}$  correspond to the anti-symmetric and symmetric stretching of  $\text{COO}^-$  vibrations of  $\text{COO}^-$  groups in citrate capped AgNPs, respectively. The broad bands in the  $3600\text{--}2800\text{ cm}^{-1}$  region correspond to the O-H stretching vibrations of the -OH groups in citrate capped AgNPs [60]. The observed peaks at  $1380\text{ cm}^{-1}$ – $1390\text{ cm}^{-1}$  belong to the vibrations of the nitro compound ( $\text{NO}_2$ ), which are produced by  $\text{AgNO}_3$  salt [61]. Ag-Ag vibrates at a wave value below  $400\text{ cm}^{-1}$  [62]. Thus, it will not be presented in Fig. 15.

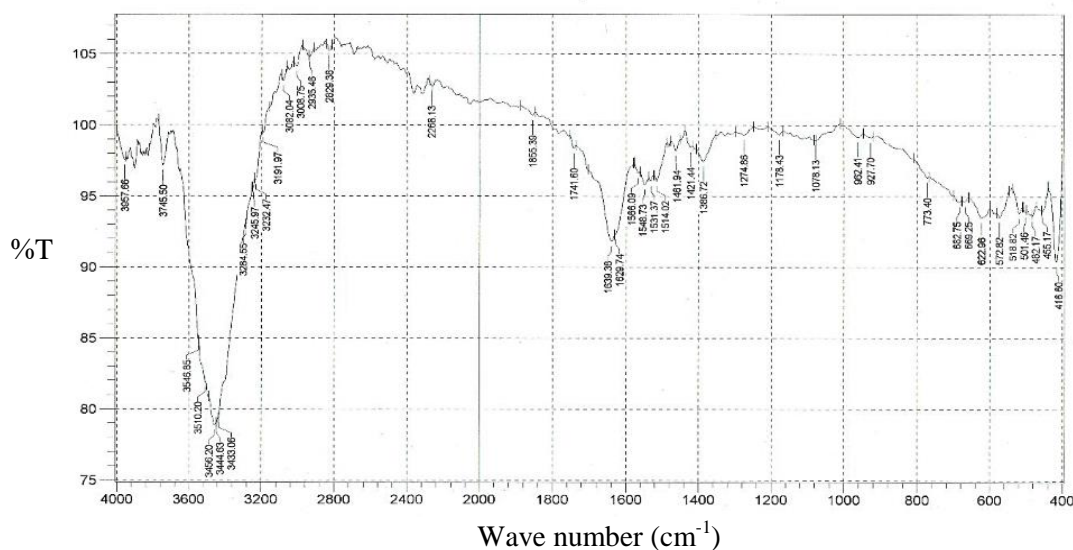


Fig. 15: FT-IR spectra of AgNPs

### 3.6 Gas test

The value resistance of the prepared thin films was converted into sensitivity  $S$  (%) using Eq. 6 (Fig. 16). A sharp increase in sensitivity was observed as the  $\text{NH}_3$  concentration rose from 50 ppm–150 ppm. This rapid response may be due to the large surface to volume ratio of the nanoneedle and the small grains of the nanostructured film. The sensitivity, response ( $\tau_{\text{res}}$ ) and recovery times ( $\tau_{\text{rec}}$ ) of C1, C2 and C3 sensor devices are listed in Table 3. The decrease in sensitivity from C3 to C1 was due to the increment in the amount of sodium (provided by the trisodium citrate) in the thin films, which increased the resistance of thin films [63] from C3 to C1.

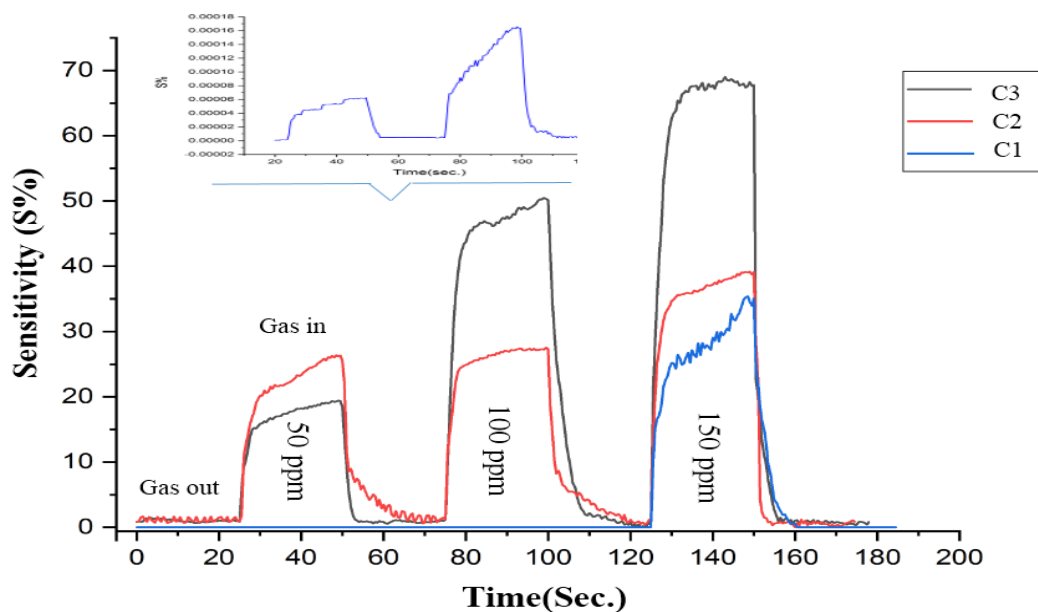


Fig.16: sensitivity of C1, C2 and C3 thin films towards (50, 100 and 150) ppm of  $\text{NH}_3$

Table. 3: The sensitivity(S%), response and recovery times of C1, C2 and C3 sensor devises

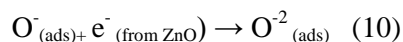
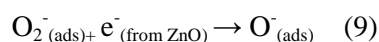
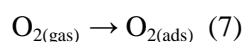
Sensor devise	Gas concentration (ppm)	Sensitivity (S%)	Response time (Sec.)	Recovery time (Sec.)
C1	50	Little	17.7	4.4
	100	Little	18.9	3.9
	150	35	20	5.7
C2	50	26	15.7	8.5
	100	27	4.2	10.3
	100	39	6.1	1.6
C3	50	19	10.9	2.2
	100	50	5.7	6.7
	150	69	5	3.6

#### 4. Proposed NH<sub>3</sub>-sensing mechanism

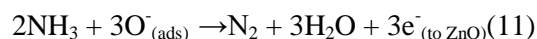
The NH<sub>3</sub> gas sensor mechanism can be summarised in three steps:

**Step 1:** Oxygen molecules in the air are adsorbed after being exposed on the Ag surface.

**Step 2:** The adsorbed oxygen molecules in Step 1 are spilled over to ZnO, wherein the molecules are converted into another oxygenated anionic form, such as O<sub>2</sub><sup>-</sup>, O<sup>-</sup> and O<sup>-2</sup>, after capturing the electrons (Eqs. 7–10) from the conduction band of ZnO, thereby increasing the value of the electrical resistance of the sensor.



**Step 3:** After the exposure of the thin films to NH<sub>3</sub>, adsorbed oxygen (O<sub>2</sub><sup>-</sup>, O<sup>-</sup> and O<sup>-2</sup>) can react with NH<sub>3</sub> molecules and break it into H<sub>2</sub>O, N<sub>2</sub> and three electrons (Eq. 11). These electrons will be transmitted into the conduction band of ZnO, thereby causing high signal given the decrease in the resistance of the sensor [64,65]. All these steps are illustrated in Fig. 17.



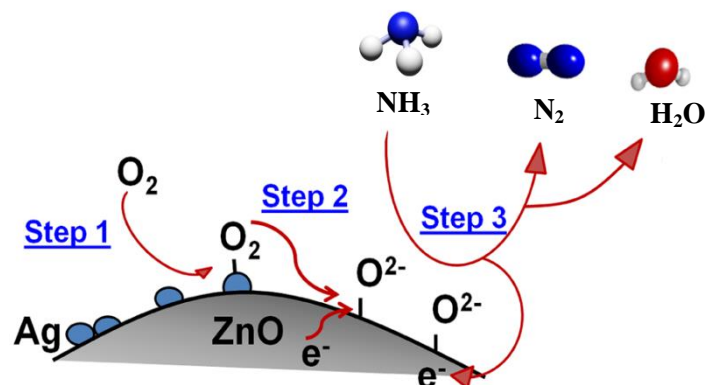


Fig. 17: Suggested steps to explain ammonia sensitivity

## 5. Conclusion

The prepared ZnO–Ag thin films showed high sensitivity (69%) to  $\text{NH}_3$  at room temperature (30 °C–33 °C). The sensitivity to  $\text{NH}_3$  gas at room temperature (30 °C–33 °C) is inversely proportional to the increased concentration of the prepared Ag nanoparticles because of the rising concentration of sodium produced from the reducing substance (e.g. sodium citrate) used for the preparation of Ag nanoparticles.

## References

1. Lim, S. H., Feng, L., Kemling, J. W., Musto, C. J., and Suslick, K. S., "An optoelectronic nose for the detection of toxic gases", *Nature Chemistry*, Vol. 1(7), 562-567 (2009).
2. Kim, J. W., Porte, Y., Ko, K. Y., Kim, H., and Myoung, J. M., "Micropatternable double-faced ZnO nanoflowers for flexible gas sensor", *ACS Applied Materials & Interfaces*, Vol. 9(38), 32876-32886 (2017).
3. Zhou, Q., Xu, L., Umar, A., Chen, W., and Kumar, R., "Pt nanoparticles decorated SnO<sub>2</sub> nanoneedles for efficient CO gas sensing applications", *Sensors and Actuators B: Chemical*, Vol. 256, 656-664 (2018).
4. Kumar, A., Sanger, A., Kumar, A., and Chandra, R., "Fast response ammonia sensors based on TiO<sub>2</sub> and NiO nanostructured bilayer thin films", *RSC Advances*, Vol. 6(81), 77636-77643 (2016).
5. Liu, X., Chen, N., Han, B., Xiao, X., Chen, G., Djerdj, I., and Wang, Y., "Nanoparticle cluster gas sensor: Pt activated SnO<sub>2</sub> nanoparticles for NH<sub>3</sub> detection with ultrahigh sensitivity", *Nanoscale*, Vol. 7(36), 14872-14880 (2015).
6. Zhang, D., Wu, J., Li, P., and Cao, Y., "Room-temperature SO<sub>2</sub> gas-sensing properties based on a metal-doped MoS<sub>2</sub> nanoflower: An experimental and density functional theory investigation", *Journal of Materials Chemistry A*, Vol. 5(39), 20666-20677 (2017).
7. Punzalan, K. B. D. B., Manalo, F. K. B., and Florido, E. A., "Ammonia gas detection using fabricated zinc oxide (ZnO) nanoparticles on glass tube substrates", In *Key Engineering Materials*. Trans Tech Publications Ltd., Vol. 775, 266-271 (2018).
8. Bateman, N., Jefferson, R., Thomas, S., Thompson, J., and Vale, A., "Oxford desk reference: toxicology". OUP Oxford, 212-217 (2014).
9. Hwang, I. S., Choi, J. K., Woo, H. S., Kim, S. J., Jung, S. Y., Seong, T. Y., and Lee, J. H., "Facile control of C<sub>2</sub>H<sub>5</sub>OH sensing characteristics by decorating discrete Ag

- nanoclusters on SnO<sub>2</sub> nanowire networks", ACS Applied Materials & Interfaces, Vol. 3(8), 3140-3145 (2011).
10. Zhang, Z., Zou, R., Song, G., Yu, L., Chen, Z., and Hu, J., "Highly aligned SnO<sub>2</sub> nanorods on graphene sheets for gas sensors", Journal of Materials Chemistry, Vol. 21(43), 17360-17365 (2011).
  11. Ghosh, A., Zhang, C., Shi, S. Q., and Zhang, H., "High-Temperature gas sensors for harsh environment applications: A review", Clean–Soil, Air, Water, Vol. 47(8), 1-33 (2019).
  12. Chen, H., Liu, Y., Xie, C., Wu, J., Zeng, D., and Liao, Y., "A comparative study on UV light activated porous TiO<sub>2</sub> and ZnO film sensors for gas sensing at room temperature", Ceramics International, Vol. 38(1), 503-509 (2012).
  13. Lee, J. H., Ko, K. H., and Park, B. O., "Electrical and optical properties of ZnO transparent conducting films by the sol–gel method", Journal of Crystal Growth, Vol. 247(1-2), 119-125 (2003).
  14. Hu, Y., Jiang, Z., Xu, C., Mei, T., Guo, J., and White, T., "Monodisperse ZnO nanodots: synthesis, characterization, and optoelectronic properties", The Journal of Physical Chemistry C, Vol. 111(27), 9757-9760 (2007).
  15. Mirzaei, A., Park, S., Kheel, H., Sun, G. J., Lee, S., and Lee, C., "ZnO-capped nanorod gas sensors", Ceramics International, Vol. 42(5), 6187-6197 (2016).
  16. Kwon, Y. J., Kang, S. Y., Mirzaei, A., Choi, M. S., Bang, J. H., Kim, S. S., and Kim, H. W., "Enhancement of gas sensing properties by the functionalization of ZnO-branched SnO<sub>2</sub> nanowires with Cr<sub>2</sub>O<sub>3</sub> nanoparticles", Sensors and Actuators B: Chemical, Vol. 249, 656-666 (2017).
  17. Powell, D. A., Kalantar-zadeh, K., and Wlodarski, W., "Numerical calculation of SAW sensitivity: Application to ZnO/LiTaO<sub>3</sub> transducers", Sensors and Actuators A: Physical, Vol. 115(2-3), 456-461 (2004).
  18. Olson, D. C., Piris, J., Collins, R. T., Shaheen, S. E., and Ginley, D. S., "Hybrid photovoltaic devices of polymer and ZnO nanofiber composites", Thin Solid Films, Vol. 496(1), 26-29 (2006).
  19. Wang, X., Zhang, J., Zhu, Z., and Zhu, J., "Effect of Pd<sup>2+</sup> doping on ZnO nanotetrapods ammonia sensor", Colloids and Surfaces A: Physicochemical and Engineering Aspects, Vol. 276(1-3), 59-64 (2006).
  20. Oh, E., Choi, H. Y., Jung, S. H., Cho, S., Kim, J. C., Lee, K. H., and Jeong, S. H., "High-performance NO<sub>2</sub> gas sensor based on ZnO nanorod grown by ultrasonic irradiation", Sensors and Actuators B: Chemical, Vol. 141(1), 239-243 (2009).
  21. Dhawale, D. S., and Lokhande, C. D., "Chemical route to synthesis of mesoporous ZnO thin films and their liquefied petroleum gas sensor performance", Journal of Alloys and Compounds, Vol. 509(41), 10092-10097 (2011).
  22. Aygün, S., and Cann, D., "Hydrogen sensitivity of doped CuO/ZnO heterocontact sensors", Sensors and Actuators B: Chemical, Vol. 106(2), 837-842 (2005).
  23. Dong, L. F., Cui, Z. L., and Zhang, Z. K., "Gas sensing properties of nano-ZnO prepared by arc plasma method", Nanostructured materials, Vol. 8(7), 815-823 (1997).
  24. Wei, A., Pan, L., and Huang, W., "Recent progress in the ZnO nanostructure-based sensors", Materials Science and Engineering: B, Vol. 176(18), 1409-1421 (2011).
  25. Wang, X., Sun, F., Duan, Y., Yin, Z., Luo, W., Huang, Y., and Chen, J., "Highly sensitive, temperature-dependent gas sensor based on hierarchical ZnO nanorod arrays", Journal of Materials Chemistry C, Vol. 3(43), 11397-11405 (2015).

26. Shi, J. P., and Harrison, R. M., "Regression modelling of hourly NO<sub>x</sub> and NO<sub>2</sub> concentrations in urban air in London", *Atmospheric Environment*, Vol. 31(24), 4081-4094 (1997).
27. Vayssieres, L., "Growth of arrayed nanorods and nanowires of ZnO from aqueous solutions", *Advanced Materials*, Vol. 15(5), 464-466 (2003).
28. Al-Hadeethi, Y., Umar, A., Ibrahim, A. A., Al-Heniti, S. H., Kumar, R., Baskoutas, S., and Raffah, B. M., "Synthesis, characterization and acetone gas sensing applications of Ag-doped ZnO nanoneedles", *Ceramics International*, Vol. 43(9), 6765-6770 (2017).
29. Xing, X., Xiao, X., Wang, L., and Wang, Y., "Highly sensitive formaldehyde gas sensor based on hierarchically porous Ag-loaded ZnO heterojunction nanocomposites", *Sensors and Actuators B: Chemical*, Vol. 247, 797-806 (2017).
30. Barthwal, S., Kim, Y., Ahn, J., and Lim, S. H., "Fabrication of a superamphiphilic SS-400 oil separator surface using a Ag-doped ZnO nanorod coating", *Science of Advanced Materials*, Vol. 8(8), 1595-1602 (2016).
31. Drmosh, Q. A., and Yamani, Z. H., "Hydrogen sensing properties of sputtered ZnO films decorated with Pt nanoparticles", *Ceramics International*, Vol. 42(10), 12378-12384 (2016).
32. Wongrat, E., Chanlek, N., Chueaiarrom, C., Thupthimchun, W., Samransuksamer, B., and Choopun, S., "Acetone gas sensors based on ZnO nanostructures decorated with Pt and Nb", *Ceramics International*, Vol. 43, S557-S566 (2017).
33. Xing, L. L., Wang, Q., and Xue, X. Y., "One-step synthesis of Pt-ZnO nanoflowers and their enhanced photocatalytic activity", *Science of Advanced Materials*, Vol. 8(6), 1275-1279 (2016).
34. Hassan, M. M., Khan, W., Mishra, P., Islam, S. S., and Naqvi, A. H., "Enhancement in alcohol vapor sensitivity of Cr doped ZnO gas sensor", *Materials Research Bulletin*, Vol. 93, 391-400 (2017).
35. Xiang, Q., Meng, G., Zhang, Y., Xu, J., Xu, P., Pan, Q., and Yu, W., "Ag nanoparticle embedded-ZnO nanorods synthesized via a photochemical method and its gas-sensing properties", *Sensors and Actuators B: Chemical*, Vol. 143(2), 635-640 (2010).
36. Patil, P. S., "Versatility of chemical spray pyrolysis technique", *Materials Chemistry and Physics*, Vol. 59(3), 185-198 (1999).
37. Tarwal, N. L., and Patil, P. S., "Superhydrophobic and transparent ZnO thin films synthesized by spray pyrolysis technique", *Applied Surface Science*, Vol. 256(24), 7451-7456 (2010).
38. Liu, M., Wei, X. Q., Zhang, Z. G., Sun, G., Chen, C. S., Xue, C. S., and Man, B. Y., "Effect of temperature on pulsed laser deposition of ZnO films", *Applied Surface Science*, Vol. 252(12), 4321-4326 (2006).
39. Tarwal, N. L., and Patil, P. S., "Enhanced photoelectrochemical performance of Ag-ZnO thin films synthesized by spray pyrolysis technique", *Electrochimica Acta*, Vol. 56(18), 6510-6516 (2011).
40. Chamberlin, R. R., and Skarman, J. S., "Chemical spray deposition process for inorganic films", *Journal of the Electrochemical Society*, Vol. 113(1), 86-89 (1966).
41. Mooney, J. B., and Radding, S. B., "Spray pyrolysis processing", *Annual Review of Materials Science*, Vol. 12(1), 81-101 (1982).

42. Dolbec, R., El Khakani, M. A., Serventi, A. M., and Saint-Jacques, R. G., "Influence of the nanostructural characteristics on the gas sensing properties of pulsed laser deposited tin oxide thin films", *Sensors and Actuators B: Chemical*, Vol. 93(1-3), 566-571 (2003).
43. Malik, O., La Hidalga-Wade, F. J. D., and Amador, R. R., "Spray pyrolysis processing for optoelectronic applications", *InTech*, 197-205 (2017).
44. Baraton, M. I., "Sensors for environment, health and security: advanced materials and technologies", *Springer Science & Business Media*, 58- 65 (2008).
45. Perednis, D., and Gauckler, L. J., "Solid oxide fuel cells with YSZ films prepared using spray pyrolysis", *ECS Proceedings Volumes*, Vol (2003), 970-975 (2003).
46. Kumar, D. S., Kumar, B. J., and Mahesh, H. M., "Quantum nanostructures (QDs): An overview", In *Synthesis of Inorganic Nanomaterials*, Woodhead Publishing, 59-88 (2018).
47. Handoko, C. T., Huda, A., and Gulo, F., " Synthesis pathway and powerful antimicrobial properties of silver nanoparticle: A critical review ", *Asian J. Sci. Res*, Vol. 12, 1-17 (2019).
48. Sadak, M. S., "Impact of silver nanoparticles on plant growth, some biochemical aspects, and yield of fenugreek plant (*Trigonella foenum-graecum*)", *Bulletin of the National Research Centre*, Vol. 43(1), 1-6 (2019).
49. Tsai, Y. T., Chang, S. J., Ji, L. W., Hsiao, Y. J., Tang, I. T., Lu, H. Y., and Chu, Y. L., "High sensitivity of NO gas sensors based on novel Ag-doped ZnO nanoflowers enhanced with a UV light-emitting diode" *ACS Omega*, Vol. 3(10), 13798-13807 (2018).
50. Vasudev, R. A. "Synthesis and characterization of nanocrystalline ZnO gas sensor (Doctoral dissertation)", *Solapur University*, 6-7 (2015).
51. Dilonardo, E., Penza, M., Alvisi, M., Cassano, G., Di Franco, C., Palmisano, F., and Cioffi, N., "Sensitive detection of hydrocarbon gases using electrochemically Pd-modified ZnO chemiresistors", *Beilstein Journal of Nanotechnology*, Vol. 8(1), 82-90 (2017).
52. Alenezi, M. R., Alshammari, A. S., Jayawardena, K. I., Beliatis, M. J., Henley, S. J., and Silva, S. R. P., "Role of the exposed polar facets in the performance of thermally and UV activated ZnO nanostructured gas sensors", *The Journal of Physical Chemistry C*, Vol. 117(34), 17850-17858 (2013).
53. Gültekin, D., Alaf, M., and Akbulut, H., "Nanostructured ZnO photo electrode synthesis for dye sensitized solar cells", *Acta Physica Polonica A*, Vol. 125(2), 301-303 (2014).
54. Vladut, C. M., Mihaiu, S., Tenea, E., Preda, S., Calderon-Moreno, J. M., Anastasescu, M., and Zaharescu, M., "Optical and piezoelectric properties of Mn-doped ZnO films deposited by sol-gel and hydrothermal methods", *Journal of Nanomaterials*, Vol. 2019, 1-12 (2019).
55. Selvaraj, V., Sagadevan, S., Muthukrishnan, L., Johan, M. R., and Podder, J., "Eco-friendly approach in synthesis of silver nanoparticles and evaluation of optical, surface morphological and antimicrobial properties", *Journal of Nanostructure in Chemistry*, Vol. 9(2), 153-162 (2019).
56. Mani, G. K., and Rayappan, J. B. B., "A highly selective room temperature ammonia sensor using spray deposited zinc oxide thin film", *Sensors and Actuators B: Chemical*, Vol. 183, 459-466 (2013).
57. Garde, A. S., "LPG and NH<sup>3</sup> Sensing Properties of SnO<sup>2</sup> thick film resistors prepared by screen printing technique", *Sensors & Transducers*, Vol. 122(11), 128-142 (2010).



58. Ismail, M., and Jabra, R., "Investigation the parameters affecting on the synthesis of silver nanoparticles by chemical reduction method and printing a conductive pattern", *J. Mater. Environ. Sci.*, Vol. 8(11), 4152-4159 (2017).
59. Shameli, K., Ahmad, M. B., Zamanian, A., Sangpour, P., Shabanzadeh, P., Abdollahi, Y., and Zargar, M., "Green biosynthesis of silver nanoparticles using *Curcuma longa* tuber powder", *International Journal of Nanomedicine*, Vol. 7, 5603-5610 (2012).
60. Pedroni, M., Piccinelli, F., Passuello, T., Polizzi, S., Ueda, J., Haro-González, P., and Speghini, A., "Water (H<sub>2</sub>O and D<sub>2</sub>O) dispersible NIR-to-NIR upconverting Yb<sup>3+</sup>/Tm<sup>3+</sup> doped MF<sub>2</sub> (M= Ca, Sr) colloids: influence of the host crystal", *Crystal Growth & Design*, Vol. 13(11), 4906-4913 (2013).
61. Sodha, K. H., Jadav, J. K., Gajera, H. P., and Rathod, K. J., "Characterization of silver nanoparticles synthesized by different chemical reduction methods", *International Journal of Pharma and Bio Sciences*, Vol. 6(4), 199-208 (2015).
62. Gharibshahi, L., Saion, E., Gharibshahi, E., Shaari, A. H., and Matori, K. A., "Structural and optical properties of Ag nanoparticles synthesized by thermal treatment method", *Materials*, Vol. 10(4), 1-13 (2017).
63. Basyooni, M. A., Shaban, M., and El Sayed, A. M., "Enhanced gas sensing properties of spin-coated Na-doped ZnO nanostructured films", *Scientific Reports*, Vol. 7, 1-12 (2017).
64. Nadargi, D. Y., Tamboli, M. S., Patil, S. S., Mulla, I. S., and Suryavanshi, S. S., "Development of Ag/ZnO nanorods and nanoplates at low hydrothermal temperature and time for acetone sensing application: an insight into spillover mechanism", *SN Applied Sciences*, Vol. 1(12), 1-10 (2019).
65. Wani, I. A., Ganguly, A., Ahmed, J., and Ahmad, T., "Silver nanoparticles: Ultrasonic wave assisted synthesis, optical characterization and surface area studies", *Materials Letters*, Vol. 65(3), 520-522 (2011).